2012 American Control Conference
Fairmont Queen Elizabeth, Montréal, Canada
June 27-June 29, 2012

Turbulent drag reduction by transverse wall oscillations

Rashad Moarref and Mihailo R. Jovanović

***Abstract*— Skin-friction drag reduction by transverse wall oscillations has received significant attention of flow control community. Both experiments and simulations have demonstrated that oscillations with properly selected amplitude and frequency can reduce turbulent drag by as much as 40 percent. For a turbulent channel flow, we develop a model-based approach to design oscillations that suppress turbulence. We show that judiciously selected linearization of the flow with control can be used to determine turbulent viscosity in a computationally efficient manner. The resulting correction to the turbulent mean velocity is then used to identify optimal frequency of oscillations, which is in close agreement with previously conducted experimental and numerical studies. This demonstrates the predictive power of our simulation-free approach to controlling turbulent flows.**

***Index Terms*— Drag reduction; flow control; stochastically forced Navier-Stokes equations; time-periodic systems; turbulence modeling.**

I. Introduction

Flow control has a potential for enhancing the efficiency and performance of engineering systems involving turbulent flows. This is because turbulence is responsible for large resistance to motion (drag) and therefore large loss of energy. Over the last two decades, a large body of experimental and numerical studies have shown the effectiveness of sensor-free flow control strategies for turbulence suppression in wall-bounded flows. For example, using high-fidelity numerical simulations [1] and experiments [2], [3], it was shown that a sustained suppression of turbulence can be achieved by transverse wall oscillations, which lead to up to 40 percent drag reduction. It was argued that a negative spanwise vorticity is induced by the wall motion, which effectively suppresses the turbulence by hampering the vortex stretching mechanism [3]. By studying the balance of power, it was further shown that a net power gain can be achieved for small amplitudes of oscillations [4]–[6].

In parallel with the above numerical and experimental studies, there has been a significant amount of effort for theoretical modeling, analysis, and control of fluid flows [7]. Most of these efforts have been focused on stability analysis and the problem of transition to turbulence. For example, it was shown that the dominant flow structures that are observed in transitional flows can be captured by studying the $\mathcal{H}_2$ norm of the flow dynamics [8]. Since the $\mathcal{H}_2$ norm quantifies the energy amplification of stochastic disturbances by the flow, reducing the $\mathcal{H}_2$ norm can be used as a control objective for preventing transition to turbulence. Based on this idea, transverse wall oscillations were designed for suppressing the kinetic energy of the fluctuations [9]. Recently, a sensor-free control strategy based on traveling waves was designed and shown to be effective in preventing transition to turbulence [10], [11].

R. Moarref and M. R. Jovanović are with the Department of Electrical and Computer Engineering, University of Minnesota, Minneapolis (e-mails: rashad@umn.edu, mihailo@umn.edu).

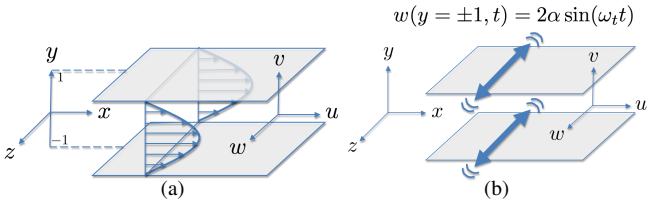

Fig. 1. (a) Pressure driven channel flow; and (b) Channel flow subject to transverse wall oscillations.

In this paper, we develop a novel model-based approach to examine the effect of transverse wall oscillations on the dynamics of a turbulent channel flow. We start by confirming that the power necessary for maintaining wall oscillations increases quadratically with their amplitude (as was first shown by [12]). This suggests that large control amplitudes may yield poor net efficiency. We thus confine our study to small oscillation amplitudes and use perturbation analysis (in the amplitude of oscillations) to identify the period of oscillations that achieves largest drag reduction in a computationally efficient manner. In addition, we quantify the net efficiency. The close agreement between our results and the results obtained in experiments and simulations demonstrates the predictive power of our model-based approach to flow control design.

Our presentation is organized as follows: We formulate the problem in Section II. The stochastically forced linearized model for evolution of fluctuations around the base turbulent flow is given in Section III. In addition, an efficient method for computing the fluctuation statistics is provided and the details of determining the influence of fluctuations on the turbulent drag are presented. Our theoretical developments are applied to the problem of turbulent drag reduction using wall oscillations in Section IV. The paper is concluded in Section V.

II. Problem formulation

Consider the pressure-driven channel flow of incompressible Newtonian fluids with geometry shown in Fig. 1(a). This flow is governed by the non-dimensional Navier-Stokes (NS) and continuity equations

$$\begin{aligned} \mathbf{u}_t &= -(\mathbf{u}\cdot\nabla)\mathbf{u} - \nabla P + (1/R_\tau)\,\Delta\mathbf{u}, \\ 0 &= \nabla\cdot\mathbf{u}, \end{aligned} \tag{1}$$

where $\mathbf{u}$ is the velocity vector, P is pressure, ∇ is the gradient, and $\Delta = \nabla \cdot \nabla$ is the Laplacian. The streamwise, wall-normal, and spanwise coordinates are represented by (x, y, z), and t denotes time. The subscripts are used to denote the spatial and temporal derivatives, e.g., $\mathbf{u}_x = \partial \mathbf{u}/\partial x = \partial_x \mathbf{u}$. The friction Reynolds number $R_\tau = u_\tau h/\nu$ is defined in terms of the channel's half-height h and the friction velocity $u_\tau = \sqrt{\tau_w/\rho}$. Here, τ_w denotes the wall-shear stress, ρ is fluid density, and ν is kinematic viscosity. In (1), length is non-dimensionalized by h, velocity by u_τ, time by h/u_τ, and pressure by ρu_τ^2.

Throughout the paper we consider the case where the bulk flux, which is obtained by integrating the streamwise velocity over spatial coordinates, remains constant. This constraint can be satisfied by adjusting the uniform streamwise pressure gradient P_x, which balances the wall-shear stress [13]. In addition to the driving pressure gradient, the flow is also subject to zero-mean transverse wall oscillations of amplitude α and frequency ω_t; see Fig. 1(b) for an illustration. The period of oscillations normalized by h/u_τ (outer units) is given by $T = 2\pi/\omega_t$, which is equivalent to $T^+ = R_\tau T$ when normalized by ν/u_τ^2 (viscous units). The streamwise and wall normal velocities satisfy no-slip and no-penetration boundary conditions at the walls.

The Reynolds decomposition of the velocity field is obtained by time-averaging [13]

$$\mathbf{u} \;=\; \mathbf{U} + \mathbf{v}, \quad \mathbf{U} \;=\; \mathcal{E}\left(\mathbf{u}\right), \quad \mathcal{E}\left(\mathbf{v}\right) \;=\; 0, \tag{2}$$

where $\mathcal{E}\left(\cdot\right)$ denotes the expectation operator, $\mathbf{U} = [\, U \; V \; W \,]^T$ is the turbulent mean velocity, and $\mathbf{v} = [\, u \; v \; w \,]^T$ is the vector of velocity fluctuations around $\mathbf{U}$. The turbulent mean velocity $\mathbf{U}$ obeys the Reynolds-averaged NS equations, which are obtained by substituting (2) into (1) and by taking the expectation

$$\begin{aligned} \mathbf{U}_t \;&=\; -\left(\mathbf{U}\cdot\nabla\right)\mathbf{U} - \nabla P + \left(1/R_\tau\right)\Delta\mathbf{U} - \nabla\cdot\mathcal{E}\left(\mathbf{v}\mathbf{v}^T\right), \\ 0 \;&=\; \nabla\cdot\mathbf{U}. \end{aligned} \tag{3}$$

Here, $\mathcal{E}\left(\mathbf{v}\mathbf{v}^T\right)$ denotes the Reynolds stress tensor which quantifies the transport of momentum arising from turbulent fluctuations [13]. Clearly, determination of mean velocity requires knowledge of the fluctuation correlations (i.e., the Reynolds stresses) which, in a turbulent flow, have profound influence on the mean flow. The difficulty stems from the fact that the nth velocity moment depends on the $(n+1)$th moment (the so-called closure problem) [13].

The closure problem in (3) can be overcome by expressing the higher order moments in terms of the lower-order moments. According to the turbulent viscosity hypothesis [13], the turbulent momentum is transported in the direction of the mean rate of strain,

$$\mathcal{E}\left(\overline{\mathbf{v}\mathbf{v}^T}\right) - \frac{1}{3}\,\mathrm{tr}\left(\mathcal{E}\left(\overline{\mathbf{v}\mathbf{v}^T}\right)\right) I \;=\; -\frac{\nu_T}{R_\tau}\,\left(\nabla\mathbf{U} + (\nabla\mathbf{U})^T\right), \tag{4}$$

where $\nu_T(y)$ is the turbulent viscosity normalized by ν, overline denotes averaging over x and z, $\mathrm{tr}(\cdot)$ is the trace of a tensor, and I is the identity operator.

A. Turbulent mean velocity

The steady-state solution of system (3)-(4) subject to a uniform pressure gradient, P_x, and transverse wall oscillations,

$$W(y \;=\; \pm 1, t) \;=\; 2\,\alpha\sin\left(\omega_t\, t\right),$$

is determined by $[\, U(y) \;\; 0 \;\; W(y,t) \,]^T$. It can be shown that U arises from the uniform pressure gradient, while W is induced by wall oscillations

$$\begin{cases} 0 \;=\; \left(\left(1+\nu_T\right)U_y\right)_y \;-\; R_\tau\, P_x, \\ U(y \;=\; \pm 1) \;=\; 0, \end{cases} \tag{5a}$$

$$\begin{cases} R_\tau\, W_t \;=\; \left(\left(1+\nu_T\right)W_y\right)_y \\ W(y \;=\; \pm 1, t) \;=\; 2\,\alpha\sin\left(\omega_t\, t\right). \end{cases} \tag{5b}$$

where $(1+\nu_T)$ represents an effective viscosity that accounts for both molecular and turbulent dissipation [14].

For given turbulent viscosity ν_T and driving pressure gradient P_x, (5) represents an uncoupled system of equations for U and W. In particular, the spanwise velocity W is periodic in time

$$W(y,t) \;=\; \alpha\left(W_1(y)\,\mathrm{e}^{\mathrm{i}\omega_t\, t} \;+\; W_1^*(y)\,\mathrm{e}^{-\mathrm{i}\omega_t\, t}\right), \tag{6}$$

where * denotes the complex conjugate, and $\mathrm{i} = \sqrt{-1}$.

The difficulty in determining U and W from (5) arises from the fact that ν_T depends on the fluctuations around the turbulent mean velocity, and thus it is not known *a priori*. A significant body of work has been devoted to finding an expression for ν_T that yields the turbulent mean velocity in the uncontrolled flow [15]

$$\begin{aligned} \nu_{T0}(y) \;=\; \frac{1}{2}\,\Bigg(\Bigg(1 \;+\; \Big(\frac{c_2}{3}\,R_\tau\left(1-y^2\right)\left(1+2y^2\right)\times \\ \left(1-e^{-(1-|y|)\,R_\tau/c_1}\right)\Big)^2\Bigg)^{1/2} - 1\Bigg). \end{aligned} \tag{7}$$

The parameters c_1 and c_2 are selected to minimize least squares deviation between the mean streamwise velocity obtained from (5a) with $P_x = -1$ and turbulent viscosity (7), and the mean streamwise velocity obtained in experiments and simulations. Application of this procedure yields $c_1 = 46.2, c_2 = 0.61$ for $R_\tau = 186$. Under the assumption that the turbulent viscosity (7) captures the effect of background turbulence on the turbulent mean veocity, the system of equations (5)-(7) yields a solution $\mathbf{U}_0 = [\, U_0(y) \;\; 0 \;\; W_0(y,t) \,]^T$. The implications of this assumption for determining the skin-friction drag coefficient and the control net efficiency are discussed in Section II-B where we show the necessity of accounting for the effect of control on the turbulent viscosity.

B. Skin-friction drag coefficient and net efficiency

As mentioned in Section II, we adjust the pressure gradient P_x in order to maintain the constant bulk flux,

$$U_B \;=\; \frac{1}{2}\int_{-1}^{1} U(y)\,\mathrm{d}y.$$

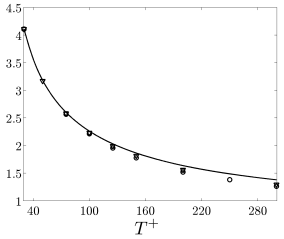

Fig. 2. The required power $\%\Pi_{\mathrm{req},0}$ as a function of the period of oscillations T^+ for the flow with $R_\tau = 186$. The symbols represent $\%\Pi_{\mathrm{req}}/\alpha^2$ obtained from the numerical simulations of [6] for $R_\tau = 200$ and three control amplitudes $\alpha = 2.25,\ \circ$; $\alpha = 6,\ \square$; and $\alpha = 9,\ \triangledown$.

Since the skin-friction drag coefficient is proportional to $|P_x|$ and inversely proportional to U_B^2 [13],

$$C_f \ = \ 2\,|P_x|/U_B^2,$$

for the flow with constant U_B, reduction (increase) in $|P_x|$ induces drag reduction (increase). The change in the skin-friction coefficient relative to the flow with no control is given by

$$\%C_f \ = \ 100\,\frac{C_{f,u} \ - \ C_{f,c}}{C_{f,u}} \ = \ 100\,(1 \ + \ P_{x,c}), \quad (8)$$

where the subscripts u and c denote the quantities in the uncontrolled and controlled flows, respectively. Thus, the control leads to drag reduction when $P_{x,c} > -1$.

The drag reduction induces saving in power (per unit area of the channel surface and normalized by ρu_τ^2) [16]

$$\Pi_{\mathrm{save}} \ = \ 2\,U_B\,(1 \ + \ P_{x,c}).$$

Compared to the power required to drive the flow with no control, $\Pi_u = 2U_B$, the saved power is determined by the relative change in the skin-friction coefficient,

$$\%\Pi_{\mathrm{save}} \ = \ 100\,\frac{\Pi_{\mathrm{save}}}{2U_B} \ = \ 100\,(1 \ + \ P_{x,c}) \ = \ \%C_f.$$

On the other hand, an input power is required for balancing the spanwise shear stresses at the walls [16]. The required power exerted by wall oscillations expressed in fraction of the power necessary to drive the uncontrolled flow is given by

$$\%\Pi_{\mathrm{req}} \ = \ 100\,\frac{\alpha^2}{R_\tau U_B}\,\mathrm{Im}\left(W_1'|_{y=-1} \ - \ W_1'|_{y=1}\right), \quad (9)$$

where $\mathrm{Im}\,(\cdot)$ denotes the imaginary part of a complex number, and prime represents differentiation with respect to y. The net efficiency of control is quantified by the difference of the saved and required powers

$$\%\Pi_{\mathrm{net}} \ = \ \%\Pi_{\mathrm{save}} \ - \ \%\Pi_{\mathrm{req}}.$$

We start by studying the implications of solutions U_0 and W_0 on the control net efficiency. For the spanwise mean velocity W_0, the required power grows quadratically with α, $\%\Pi_{\mathrm{req}} = \alpha^2\,\%\Pi_{\mathrm{req},0}$. The solid curve in Fig. 2 shows $\%\Pi_{\mathrm{req},0}(T^+)$ for $R_\tau = 186$. We see that the required power is a monotonically decreasing function of T^+. Therefore, in view of net efficiency, the optimum period of oscillations may be larger than the period that yields maximum drag reduction. The symbols in Fig. 2 show close correspondence between $\%\Pi_{\mathrm{req},0}$ and the results obtained from numerical simulations [6].

The apparent lack of influence of the wall movements on U_0, observed in Section II-A, is at odds with experiments and simulations that have shown that properly designed oscillations can reduce drag by as much as 40%. Thus, model-based control of turbulent flows requires thorough examination of the influence of control on ν_T.

C. The model equation for ν_T

The challenge here is to establish a relation between ν_T and the second-order statistics of velocity fluctuations. Using dimensional analysis a model equation for turbulent viscosity is given by [14]

$$\nu_T(y) \ = \ c\,R_\tau^2\,\frac{k(y)^2}{\epsilon(y)}, \quad (10)$$

where k is the turbulent kinetic energy, ϵ is the its rate of dissipation and $c = 0.09$. Both k and ϵ are determined by the second-order statistics of fluctuations averaged over the horizontal directions and one period T

$$\begin{aligned} k(y) \ &= \ \frac{1}{2T}\int_0^T \mathcal{E}\,(\overline{uu} \ + \ \overline{vv} \ + \ \overline{ww})\,(y,t)\,\mathrm{d}t, \\ \epsilon(y) \ &= \ \frac{1}{T}\int_0^T \mathcal{E}\,(2\,(\overline{u_x\,u_x} \ + \ \overline{v_y\,v_y} \ + \ \overline{w_z\,w_z} \ + \ \overline{u_y\,v_x} \ + \\ &\qquad \overline{u_z\,w_x} \ + \ \overline{v_z\,w_y}) \ + \ \overline{u_y\,u_y} \ + \ \overline{w_y\,w_y} \ + \\ &\qquad \overline{v_x\,v_x} \ + \ \overline{w_x\,w_x} \ + \ \overline{u_z\,u_z} \ + \ \overline{v_z\,v_z})\ (y,t)\,\mathrm{d}t. \end{aligned} \quad (11)$$

We next develop a computationally efficient method, that is amenable to control design, for determining the effect of actuation on ν_T.

III. Stochastically forced flow with control

Since ν_T in (10) is determined by the second-order statistics of velocity fluctuations, we use *stochastically forced linearized NS equations* to compute k and ϵ in the flow with control. Here, we utilize the fact that the second-order statistics of linear time-periodic systems can be obtained from the solution of the corresponding Lyapunov equation [17]. It is well-known that the analysis of the steady-state variance of infinitesimal fluctuations around the laminar flow can be used to identify flow structures that initiate the onset of turbulence [8], [18], [19]. In this paper, we show that judiciously selected linearization of the turbulent flow with control can be used to approximate the turbulent viscosity in a computationally efficient way.

Next, we examine the effect of control on small-amplitude fluctuations around $\mathbf{U}_0 = [\,U_0(y)\ 0\ W_0(y,t)\,]^T$. An equivalent expression for $\mathbf{U}_0$ can be found from the periodic steady-state solution of the turbulent-viscosity-enhanced NS

equations subject to wall-oscillations,

$$\begin{aligned}\mathbf{u}_t &= -(\mathbf{u}\cdot\nabla)\,\mathbf{u} - \nabla P + \\ &\quad (1/R_\tau)\,\nabla\cdot\big((1+\nu_{T0})\,\big(\nabla\mathbf{u} + (\nabla\mathbf{u})^T\big)\big), \\ 0 &= \nabla\cdot\mathbf{u}.\end{aligned}$$

Our simulation-free design of drag-reducing transverse oscillations involves four steps:

(i) *the turbulent mean velocity in the presence of control is obtained from (5) where closure is achieved using the turbulent viscosity of the uncontrolled flow (7)*;
(ii) *k and ϵ are determined from the second-order statistics of fluctuations that are obtained from the stochastically forced NS equations linearized around the turbulent mean velocity determined in* (i);
(iii) *for the flow with control, the modifications to k and ϵ are used to determine the modification to the turbulent viscosity, ν_T*;
(iv) *the modified ν_T is used in (5) to determine the effect of fluctuations on the mean velocity, and thereby skin-friction drag and control net efficiency*.

The Fourier transform in x and z brings the NS equations (with turbulent viscosity) linearized around $\mathbf{U}_0 = [\,U_0(y)\;0\;W_0(y,t)\,]^T$ to an evolution form parameterized by the streamwise and spanwise wavenumbers $\boldsymbol{\kappa} = (\kappa_x,\,\kappa_z)$

$$\begin{aligned}\boldsymbol{\psi}_t(y,\boldsymbol{\kappa},t) &= A(\boldsymbol{\kappa},t)\,\boldsymbol{\psi}(y,\boldsymbol{\kappa},t) + \mathbf{f}(y,\boldsymbol{\kappa},t), \\ \mathbf{v}(y,\boldsymbol{\kappa},t) &= C(\boldsymbol{\kappa})\,\boldsymbol{\psi}(y,\boldsymbol{\kappa},t).\end{aligned} \tag{12}$$

Here, $\boldsymbol{\psi} = [\,v\;\;\eta\,]^T$ is the state, $\eta = \mathrm{i}\kappa_z u - \mathrm{i}\kappa_x w$ is the wall-normal vorticity, and $\mathbf{f}$ is the stochastic forcing. The same symbol is used to denote the variables in both physical and wavenumber domains (these cases are distinguished from the context). System (12) represents a family of PDEs in y and t with time-periodic coefficients. The operators A and C in (12) are given by

$$\begin{aligned}A &= \begin{bmatrix} A_{11} & 0 \\ A_{21} & A_{22}\end{bmatrix}, \\ A_{11} &= \Delta^{-1}\big(((1+\nu_{T0})/R_\tau)\Delta^2 + (2\nu'_{T0}/R_\tau)\Delta\partial_y + \\ &\quad (\nu''_{T0}/R_\tau)(\partial_y^2+\kappa^2) + \\ &\quad \mathrm{i}\kappa_x\big(U_0''-U_0\Delta\big) + \mathrm{i}\kappa_z\big(W_0''-W_0\Delta\big)\big), \\ A_{21} &= -\mathrm{i}\kappa_z U_0' + \mathrm{i}\kappa_x W_0', \\ A_{22} &= ((1+\nu_{T0})/R_\tau)\Delta + (\nu'_{T0}/R_\tau)\partial_y - \\ &\quad \mathrm{i}\kappa_x U_0 - \mathrm{i}\kappa_z W_0, \\ C &= \begin{bmatrix} C_u \\ C_v \\ C_w\end{bmatrix} = \frac{1}{\kappa^2}\begin{bmatrix} \mathrm{i}\kappa_x\partial_y & -\mathrm{i}\kappa_z \\ \kappa^2 & 0 \\ \mathrm{i}\kappa_z\partial_y & \mathrm{i}\kappa_x\end{bmatrix},\end{aligned} \tag{13}$$

where $\Delta = \partial_y^2 - \kappa^2$ is the Laplacian, $\Delta^2 = \partial_y^4 - 2\kappa^2\,\partial_y^2 + \kappa^4$, $\kappa^2 = \kappa_x^2 + \kappa_z^2$, and $\{v(\pm1,\boldsymbol{\kappa},t) = v'(\pm1,\boldsymbol{\kappa},t) = \eta(\pm1,\boldsymbol{\kappa},t) = 0\}$.

A. Computing the velocity correlations

We next briefly describe a method for determining the steady-state statistics of the linearized system (12) driven by a zero-mean temporally white stochastic forcing, with second-order statistics,

$$\mathcal{E}\,(\mathbf{f}(\,\cdot\,,\boldsymbol{\kappa},t_1)\otimes\mathbf{f}(\,\cdot\,,\boldsymbol{\kappa},t_2)) = M(\boldsymbol{\kappa})\,\delta(t_1-t_2). \tag{14}$$

Here, δ is the Dirac delta function, $\mathbf{f}\otimes\mathbf{f}$ is the tensor product of $\mathbf{f}$ with itself, and $M(\boldsymbol{\kappa})$ is a spatial spectral-density of forcing. For homogeneous isotropic turbulence, the steady-state velocity correlation tensors can be reproduced by the linearized NS equations subject to white-in-time forcing with second-order statistics proportional to the turbulent energy spectrum [20]. Using this analogy, we select $M(\boldsymbol{\kappa})$ to guarantee equivalence between the two-dimensional energy spectra of the uncontrolled turbulent flow and the flow governed by stochastically forced NS equations linearized around $\mathbf{U}_0 = [\,U_0(y)\;0\;0\,]^T$. To this end, we use the energy spectrum of the uncontrolled flow obtained from numerical simulations [21], $E(y,\boldsymbol{\kappa})$, to define

$$\begin{aligned}M(\boldsymbol{\kappa}) &= \frac{\bar{E}(\boldsymbol{\kappa})}{\bar{E}_0(\boldsymbol{\kappa})}\,M_0(\boldsymbol{\kappa}), \\ M_0(\boldsymbol{\kappa}) &= \begin{bmatrix}\sqrt{E}\,I & 0 \\ 0 & \sqrt{E}\,I\end{bmatrix}\begin{bmatrix}\sqrt{E}\,I & 0 \\ 0 & \sqrt{E}\,I\end{bmatrix}^+.\end{aligned}$$

Here, $\bar{E}(\boldsymbol{\kappa}) = \int_{-1}^{1} E(y,\boldsymbol{\kappa})\,\mathrm{d}y$ is the two-dimensional energy spectrum of the uncontrolled flow, $\bar{E}_0(\boldsymbol{\kappa})$ is the energy spectrum obtained from the linearized NS equations subject to a white-in-time forcing $\mathbf{f}$ with spatial spectrum $M_0(\boldsymbol{\kappa})$, and $^+$ denotes the adjoint of an operator.

For the time-periodic system (12), the operator A in (13) can be written as

$$A(\boldsymbol{\kappa},t) = A_0(\boldsymbol{\kappa}) + \alpha\left(A_{-1}(\boldsymbol{\kappa})\,\mathrm{e}^{-\mathrm{i}\,\omega_t\,t} + A_1(\boldsymbol{\kappa})\,\mathrm{e}^{\mathrm{i}\,\omega_t\,t}\right).$$

It is a standard fact that the output of the linear time-periodic system (12) subject to a stationary input is a cyclo-stationary process [22], meaning that the statistical properties of the output are periodic in time. For example,

$$\begin{aligned}X(\boldsymbol{\kappa},t) &= \mathcal{E}\,(\boldsymbol{\psi}(\,\cdot\,,\boldsymbol{\kappa},t)\otimes\boldsymbol{\psi}(\,\cdot\,,\boldsymbol{\kappa},t)) = \\ &\quad X_0(\boldsymbol{\kappa}) + X_1(\boldsymbol{\kappa})\,\mathrm{e}^{\mathrm{i}\,\omega_t\,t} + X_1^+(\boldsymbol{\kappa})\,\mathrm{e}^{-\mathrm{i}\,\omega_t\,t} + \\ &\quad X_2(\boldsymbol{\kappa})\,\mathrm{e}^{\mathrm{i}\,2\,\omega_t\,t} + X_2^+(\boldsymbol{\kappa})\,\mathrm{e}^{-\mathrm{i}\,2\,\omega_t\,t} + \ldots.\end{aligned}$$

The averaged effect of forcing (over one period T) on the velocity correlations is determined by X_0

$$\frac{1}{T}\int_0^T X(\boldsymbol{\kappa},t)\,\mathrm{d}t = X_0(\boldsymbol{\kappa}). \tag{15}$$

In the remainder of the paper, we consider small amplitude of wall oscillations α. This choice is motivated by the observation that the power required to maintain the oscillations increases quadratically with α (cf. (9)). Thus, using large amplitudes may be prohibitively expensive from control expenditure point of view. Furthermore, for sufficiently small value of α the velocity correlations can be computed efficiently using perturbation analysis in α [17]. Up to a

second order in α, X_0 in (15) can be written as a perturbation series [9], [17]

$$X_0(\boldsymbol{\kappa}) \;=\; X_{0,0}(\boldsymbol{\kappa}) \,+\, \alpha^2\, X_{0,2}(\boldsymbol{\kappa}) \,+\, \mathcal{O}(\alpha^4), \qquad (16)$$

where the operators $X_{0,0}$ and $X_{0,2}$ are obtained from a set of decoupled Lyapunov equations [9], [17].

B. Influence of fluctuations on turbulent viscosity

According to (10), ν_T is determined by the second-order statistics of velocity fluctuations. By considering dynamics of infinitesimal fluctuations, these statistics can be obtained from the auto-correlation operator X_0. From (16), it follows

$$\begin{aligned} k \;&=\; k_0 \,+\, \alpha^2\, k_2 \,+\, \mathcal{O}(\alpha^4), \\ \epsilon \;&=\; \epsilon_0 \,+\, \alpha^2\, \epsilon_2 \,+\, \mathcal{O}(\alpha^4). \end{aligned} \qquad (17)$$

Here, the subscript 0 denotes the corresponding quantities in the uncontrolled turbulent flow, and the subscript 2 quantifies the influence of fluctuations in the controlled flow at the level of α^2. A computationally efficient method for determining k_2 and ϵ_2 from $X_{0,2}$ is provided in Appendix I.

For small amplitude oscillations, substituting k and ϵ from (17) into (10) yields

$$\nu_T \;=\; c\, R_\tau^2\, \frac{k^2}{\epsilon} \;=\; c\, R_\tau^2\, \frac{\left(k_0 + \alpha^2 k_2 + \mathcal{O}(\alpha^4)\right)^2}{\epsilon_0 + \alpha^2 \epsilon_2 + \mathcal{O}(\alpha^4)},$$

which using Neumann series expansion leads to

$$\begin{aligned} \nu_T \;&=\; \nu_{T0} \,+\, \alpha^2\, \nu_{T2} \,+\, \mathcal{O}(\alpha^4), \\ \nu_{T2} \;&=\; \nu_{T0} \left(\frac{2k_2}{k_0} \,-\, \frac{\epsilon_2}{\epsilon_0} \right). \end{aligned} \qquad (18)$$

Therefore, up to second order in α, the influence of fluctuations on turbulent viscosity in the flow with control is determined by second-order corrections to the kinetic energy k_2 and its rate of dissipation ϵ_2.

C. Skin-friction drag coefficient and net efficiency

We next show how velocity fluctuations in the flow subject to small amplitude oscillations modify the skin-friction drag coefficient and the net efficiency. As discussed in Section II-B, C_f is determined by U and $\%\Pi_{\rm net}$ is determined by both U and W. The influence of fluctuations on U in the flow with control can be obtained by substituting ν_T from (18) into (5), and thereby expressing U and P_x as

$$\begin{aligned} U \;&=\; U_0 \,+\, \alpha^2\, U_2 \,+\, \mathcal{O}(\alpha^4), \\ P_x \;&=\; -1 \,+\, \alpha^2\, P_{x,2} \,+\, \mathcal{O}(\alpha^4). \end{aligned} \qquad (19)$$

An expression for the saved power is obtained by substituting P_x from (19) into (8)

$$\%C_f \;=\; \%\Pi_{\rm save} \;=\; \alpha^2\, \%\Pi_{\rm save,2} \,+\, \mathcal{O}(\alpha^4),$$

where $\%\Pi_{\rm save,2} = 100 P_{x,2}$. Therefor, a positive (negative) value of $\%\Pi_{\rm save,2}$ signifies drag reduction (increase). Finally, the net efficiency is given by

$$\%\Pi_{\rm net} \;=\; \alpha^2\, \%\Pi_{\rm net,2} \,+\, \mathcal{O}(\alpha^4),$$

where $\%\Pi_{\rm net,2} = \%\Pi_{\rm save,2} - \%\Pi_{\rm req,0}$.

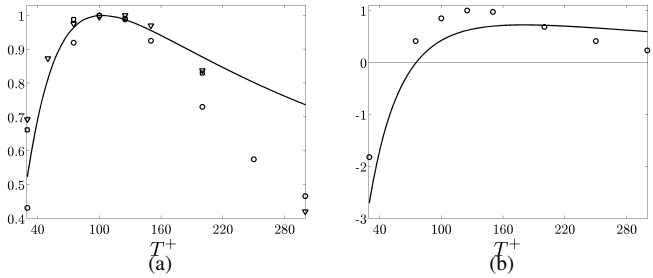

Fig. 3. (a) Comparison between second order correction to the saved power $\%\Pi_{\rm save,2}(T^+)$ for the flow with $R_\tau = 186$ (solid curve), and $\%\Pi_{\rm save}$ obtained from numerical simulations (symbols) [6] for $R_\tau = 200$ and three control amplitudes $\alpha = 2.25$, $\circ$; $\alpha = 6$, $\square$; and $\alpha = 9$, $\triangledown$. The data in (a) are normalized by their largest values; (b) Comparison between second-order correction to the net efficiency $\%\Pi_{\rm net,2}(T^+)$ (solid curve) for the flow with $R_\tau = 186$ (solid curve), and $\%\Pi_{\rm net}/\alpha^2$ obtained from numerical simulations (symbols) [6] for $R_\tau = 200$ and $\alpha = 2.25$, $\circ$.

IV. Turbulent drag reduction

We study turbulent drag reduction by transverse wall oscillations in channel flows with $R_\tau = 186$. The turbulent statistics in the channel flow with no control are provided by high-fidelity numerical simulations for this Reynolds number [21]. We use this database to obtain the turbulent energy spectrum which is used for determining the spectrum of the stochastic forcing in the evolution model; see (14). In addition, k_0 in the uncontrolled flow is extracted from this database, ν_{T0} is obtained from (7), and ϵ_0 is determined from $\epsilon_0 = c R_\tau^2\, k_0^2/\nu_{T0}$.

The differential operators are discretized in the wall-normal direction using 101 Chebyshev collocation points [23]. In x and z directions, the differential operators are algebraized using 50 and 51 Fourier wavenumbers with $0.01 < \kappa_x < 42.5$ and $0.01 < \kappa_z < 84.5$, where the largest values of κ_x and κ_z are equal to those in [21].

The solid curve in Fig. 3(a) shows the second order correction (in α) to the saved power $\%\Pi_{\rm save,2}(T^+)$ for the controlled flow with $R_\tau = 186$. The positive value of $\%\Pi_{\rm save,2}$ indicates that drag is reduced for all values of $30 < T^+ < 300$. The largest drag reduction takes place for $T^+ = 102.5$, which agrees closely with the results obtained from high-fidelity numerical simulations (symbols) [6] for $R_\tau = 200$. The quantitative differences can be attributed to the effect of higher order corrections. Another factor that warrants further scrutiny is modeling of the spatial spectrum of stochastic forcing. Analysis of these effects is beyond the scope of the current study.

The solid curve in Fig. 3(b) shows the second-order correction to the net efficiency, $\%\Pi_{\rm net,2}(T^+)$, in the flow with $R_\tau = 186$. We see that $\%\Pi_{\rm net,2} > 0$ for $T^+ > 75$, indicating that, for small control amplitudes, a positive net efficiency can be achieved if the period of oscillations is large enough. Our prediction is in close agreement with numerical simulations at $R_\tau = 200$ [6] where positive net efficiency of oscillations with $\alpha = 2.25$ is obtained for $T^+ > 70$.

V. Concluding remarks

This paper has introduced a model-based approach to controlling turbulent flows. In contrast to standard practice that embeds turbulence models in numerical simulations, we have developed a simulation-free approach that enables computationally-efficient control design and optimization. We have shown that the study of dynamics is of prime importance in designing drag-reducing wall oscillations. This has allowed us to determine the influence of control on the turbulent viscosity in a simulation-free manner. The first step in our control-oriented modeling involves augmentation of the molecular viscosity with the turbulent viscosity of the flow with no control. The resulting model is then used to determine the turbulent mean velocity in the flow with control, and to study the dynamics of velocity fluctuations around it. By considering linearized equations in the presence of white-in-time stochastic forcing (whose spatial spectrum is selected to be proportional to the turbulent kinetic energy of the flow with no control), we have quantified the influence of control on the second-order statistics of velocity fluctuations and thereby on the turbulent viscosity. Finally, the modifications to the turbulent viscosity determine the turbulent mean velocity and skin-friction drag in the flow with control. We have shown that perturbation analysis up to second order reliably predicts the optimal period of drag-reducing oscillations. We expect that our model-based approach will find use in designing other feedback-based and sensor-less turbulence suppression strategies.

Acknowledgments

Financial support from the National Science Foundation under CAREER Award CMMI-06-44793 and the University of Minnesota IREE Award RC-0014-11 are gratefully acknowledged. The Minnesota Supercomputing Institute is acknowledged for providing computational resources.

Appendix I
Computing the modifications k_2 and ϵ_2 to k and ϵ

We show that the averaged effect (over one period T) of fluctuations around the mean velocity on k_2 and ϵ_2 can be obtained from $X_{0,2}(\boldsymbol{\kappa})$. Following (11) and (16), the kinetic energy of fluctuations and its rate of dissipation are given by

$$k_2(y) = \int_{\boldsymbol{\kappa}} \mathcal{K}_k(y,y,\boldsymbol{\kappa})\,\mathrm{d}\boldsymbol{\kappa},$$
$$\epsilon_2(y) = \int_{\boldsymbol{\kappa}} \mathcal{K}_\epsilon(y,y,\boldsymbol{\kappa})\,\mathrm{d}\boldsymbol{\kappa},$$

where $\mathcal{K}_k(y,\xi,\boldsymbol{\kappa})$ and $\mathcal{K}_\epsilon(y,\xi,\boldsymbol{\kappa})$ are the kernel representation of the operators $\mathcal{N}_k$ and $\mathcal{N}_\epsilon$, respectively

$$\mathcal{N}_k(\boldsymbol{\kappa}) = \left(C_u\,X_{0,2}\,C_u^+ + C_v\,X_{0,2}\,C_v^+ + C_w\,X_{0,2}\,C_w^+\right)/2,$$

$$\begin{aligned}\mathcal{N}_\epsilon(\boldsymbol{\kappa}) = 2\,\big(&\kappa_x^2\,C_u\,X_{0,2}\,C_u^+ + \partial_y\,C_v\,X_{0,2}\,C_v^+\,\partial_y^+ + \\ &\kappa_z^2\,C_w\,X_{0,2}\,C_w^+ - \mathrm{i}\kappa_x\,\partial_y\,C_u\,X_{0,2}\,C_v^+ + \\ &\kappa_x\kappa_z\,C_u\,X_{0,2}\,C_w^+ + \mathrm{i}\kappa_z\,C_v\,X_{0,2}\,C_w^+\,\partial_y^+\big) + \\ &\partial_y\,C_u\,X_{0,2}\,C_u^+\,\partial_y^+ + \partial_y\,C_w\,X_{0,2}\,C_w^+\,\partial_y^+ + \\ &\kappa^2\,C_v\,X_{0,2}\,C_v^+ + \kappa_x^2\,C_w\,X_{0,2}\,C_w^+ + \\ &\kappa_z^2\,C_u\,X_{0,2}\,C_u^+.\end{aligned}$$

References

[1] W. Jung, N. Mangiavacchi, and R. Akhavan, "Suppression of turbulence in wall-bounded flows by high-frequency spanwise oscillations," *Phys. Fluids A*, vol. 4, no. 8, pp. 1605–1607, 1992.

[2] F. Laadhari, L. Skandaji, and R. Morel, "Turbulence reduction in a boundary layer by a local spanwise oscillating surface," *Phys. Fluids*, vol. 6, no. 10, pp. 3218–3220, 1994.

[3] K.-S. Choi, "Near-wall structure of turbulent boundary layer with spanwise-wall oscillation," *Phys. Fluids*, vol. 14, no. 7, pp. 2530–2542, 2002.

[4] A. Baron and M. Quadrio, "Turbulent drag reduction by spanwise wall oscillations," *Appl. Sci. Res.*, vol. 55, no. 4, pp. 311–326, 1996.

[5] M. Quadrio and P. Ricco, "Initial response of a turbulent channel flow to spanwise oscillation of the walls," *J. Turbul.*, no. 4, p. 007, 2003.

[6] M. Quadrio and P. Ricco, "Critical assessment of turbulent drag reduction through spanwise wall oscillations," *J. Fluid Mech.*, vol. 521, pp. 251–271, 2004.

[7] J. Kim and T. R. Bewley, "A linear systems approach to flow control," *Annu. Rev. Fluid Mech.*, vol. 39, pp. 383–417, 2007.

[8] M. R. Jovanović and B. Bamieh, "Componentwise energy amplification in channel flows," *J. Fluid Mech.*, vol. 534, pp. 145–183, July 2005.

[9] M. R. Jovanović, "Turbulence suppression in channel flows by small amplitude transverse wall oscillations," *Phys. Fluids*, vol. 20, no. 1, p. 014101, January 2008.

[10] R. Moarref and M. R. Jovanović, "Controlling the onset of turbulence by streamwise traveling waves. Part 1: Receptivity analysis," *J. Fluid Mech.*, vol. 663, pp. 70–99, November 2010.

[11] B. Lieu, R. Moarref, and M. R. Jovanović, "Controlling the onset of turbulence by streamwise traveling waves. Part 2: Direct numerical simulations," *J. Fluid Mech.*, vol. 663, pp. 100–119, November 2010.

[12] P. Ricco and M. Quadrio, "Wall-oscillation conditions for drag reduction in turbulent channel flow," *Int. J. Heat Mass Transf.*, vol. 29, no. 4, pp. 891–902, 2008.

[13] W. D. McComb, *The Physics of Fluid Turbulence*. Oxford University Press Inc., 1991.

[14] S. B. Pope, *Turbulent flows*. Cambridge University Press, 2000.

[15] W. C. Reynolds and W. G. Tiederman, "Stability of turbulent channel flow with application to Malkus's theory," *J. Fluid Mech.*, vol. 27, no. 2, pp. 253–272, 1967.

[16] I. G. Currie, *Fundamental Mechanics of Fluids*. CRC Press, 2003.

[17] M. R. Jovanović and M. Fardad, "H_2 norm of linear time-periodic systems: a perturbation analysis," *Automatica*, vol. 44, no. 8, pp. 2090–2098, August 2008.

[18] B. F. Farrell and P. J. Ioannou, "Stochastic forcing of the linearized Navier-Stokes equations," *Phys. Fluids A*, vol. 5, no. 11, pp. 2600–2609, 1993.

[19] B. Bamieh and M. Dahleh, "Energy amplification in channel flows with stochastic excitation," *Phys. Fluids*, vol. 13, no. 11, pp. 3258–3269, 2001.

[20] M. R. Jovanović and T. T. Georgiou, "Reproducing second order statistics of turbulent flows using linearized navier-stokes equations with forcing," *Bulletin of the American Physical Society*, vol. 55, 2010.

[21] J. C. del Alamo, J. Jiménez, P. Zandonade, and R. D. Moser, "Scaling of the energy spectra of turbulent channels," *J. Fluid Mech.*, vol. 500, no. 1, pp. 135–144, 2004.

[22] W. A. Gardner, *Introduction to Random Processes: with applications to signals and systems*. McGraw-Hill, 1990.

[23] J. A. C. Weideman and S. C. Reddy, "A MATLAB differentiation matrix suite," *ACM Transactions on Mathematical Software*, vol. 26, no. 4, pp. 465–519, December 2000.